

CURVATURE EFFECTS IN GAMMA-RAY BURST COLLIDING SHELLS

CHARLES D. DERMER

E. O. Hulburt Center for Space Research, Code 7653, Naval Research Laboratory, Washington, DC 20375-5352;
 dermer@gamma.nrl.navy.mil

Received 2004 March 21; accepted 2004 May 12

ABSTRACT

An elementary kinematic model for emission produced by relativistic spherical colliding shells is studied. The case of a uniform blast-wave shell with jet opening angle $\theta_j \gg 1/\Gamma$ is considered, where Γ is the Lorentz factor of the emitting shell. The shell, with comoving width $\Delta r'$, is assumed to be illuminated for a comoving time $\Delta t'$ and to radiate a broken-power-law νL_ν spectrum peaking at comoving photon energy $\epsilon'_{\text{pk},0}$. Synthetic gamma-ray burst (GRB) pulses are calculated, and the relation between energy flux and internal comoving energy density is quantified. Curvature effects dictate that the measured νF_ν flux at the measured peak photon energy ϵ_{pk} be proportional to ϵ_{pk}^3 in the declining phase of a GRB pulse. Possible reasons for discrepancies with observations are discussed, including adiabatic and radiative cooling processes that extend the decay timescale, a nonuniform jet, and the formation of pulses by external shock processes. A prediction of a correlation between prompt emission properties and times of the optical afterglow beaming breaks is made for a cooling model, which can be tested with *Swift*.

Subject headings: gamma rays: bursts — gamma rays: theory — radiation mechanisms: nonthermal

1. INTRODUCTION

In the collapsar scenario for gamma-ray bursts (GRBs), pulses in GRB light curves are thought to be produced by collisions between relativistic shells ejected from a central engine (see Zhang & Mészáros 2004 for a recent review). The interception of a more slowly moving shell by a second shell that is ejected at a later time, but with faster speed and larger Lorentz factor, produces a shock that dissipates internal energy to energize the particles that emit the GRB radiation. This scenario is widely considered to explain pulses in GRB light curves (Kobayashi et al. 1997; Daigne & Mochkovitch 1998). Studies of pulses are important for deciding whether GRB sources require engines that are long-lasting or impulsive (Dermer & Mitman 2004), with important implications for the nature of the central engine, which is often argued to be a newly formed black hole powered by the accretion of a massive, dense torus.

Here we construct an elementary kinematic model for colliding shells, assumed spherical and uniform within jet opening angle θ_j . This is the sort of jet that Frail et al. (2001) discuss regarding the standard energy reservoir result, where jet opening angles are inferred from the time of achromatic spectral breaks in optical afterglow light curves.

We also perform this study in order to quantify the curvature constraint of a spherically emitting shell traveling with bulk Lorentz factor Γ , which implies that the shell radius

$$r \approx 2\Gamma^2 c t_{\text{var}} / (1 + z) \quad (1)$$

in order to produce variability on timescale t_{var} (Rybicki & Lightman 1979; Fenimore et al. 1996). This study also quantifies both the rate at which flux decays at a given energy as a result of curvature effects and the range of validity of the approximate relation

$$\Phi_E \cong c r^2 u'_0 \Gamma^2 / d_L^2 \quad (2)$$

between internal comoving energy density u'_0 and observed energy flux Φ_E , where d_L is the luminosity distance (see Appendix A). The accuracy of this relation is important in quantifying $\gamma\gamma$ opacity constraints (Lithwick & Sari 2001; Dermer 2004) applied to GRB pulses as measured with the GRB monitor and Large Area Detector on *GLAST*,¹ as well as in making estimates of photomeson production in GRB blast waves (Waxman & Bahcall 1997).

If curvature effects dominate the late-time emission in GRB pulses, then a unique relation is found whereby the value of the νF_ν peak flux $f_{\epsilon_{\text{pk}}}$ (in cgs units of $\text{ergs cm}^{-2} \text{s}^{-1}$) at peak photon energy ϵ_{pk} decays $\propto \epsilon_{\text{pk}}^3$. This relation is generally not observed in long, smooth GRB pulses studied by Borgonovo & Ryde (2001), who find power-law decays $f_{\epsilon_{\text{pk}}} \propto \epsilon_{\text{pk}}^\zeta$, with $0.6 \lesssim \zeta \lesssim 3$. Remarkably, values of ζ for different pulses within the same GRB are confined to a rather narrow band. The wide range of values of ζ is found not only in multi-peaked GRBs, but also in single-peaked GRBs that display smooth fast-rise, slow-decay light curves (Borgonovo & Ryde 2001; Ryde & Petrosian 2002). The smooth single-peak GRBs could arise from curvature effects (Fenimore et al. 1996) or external shocks (Dermer et al. 1999a). For GRB pulses that could be produced by spherically symmetric shell collisions, the discrepancy with observations suggest a breakdown of our assumptions.

In the next section, the kinematic model is presented. Calculations based on this model are presented in § 3. In § 4, we discuss the possibility that radiative cooling effects produce the power-law relation, implying a prediction that can be tested with *Swift*.² Alternately, the uniform spherical shell assumption could break down, or the basic model of colliding shells could be in error. The appendices give derivations of simple, widely used approximations related to this study, a derivation of the curvature relation $f_{\epsilon_{\text{pk}}} \propto \epsilon_{\text{pk}}^3$, and an analytic form for the time-dependent pulse profile, leading to a simple expression for the

¹ See <http://glast.gsfc.nasa.gov>.

² See <http://swift.gsfc.nasa.gov>.

light curve of a pulse in the curvature limit. A brief summary is given in § 5.

2. KINEMATIC MODEL

A simple kinematic model for the received flux from the illumination of a spherically symmetric shell resulting from shell collisions is studied. A shell with finite width is assumed to be uniformly illuminated throughout its volume for a fixed duration during which the shell travels with constant speed from the explosion center. Light-travel time and Doppler effects are treated without regard to details of the energization and cooling of the radiating particles. This approach gives kinematic expectations of curvature effects in a GRB colliding shell system.

The νF_ν flux measured at dimensionless photon energy $\epsilon = h\nu/m_e c^2$ and time t is given by

$$f_\epsilon(t) = \frac{1}{d_L^2} \int_0^{2\pi} d\phi \int_{-1}^1 d\mu \int_0^\infty dr r^2 \delta_D^3(\mathbf{r}) \times \epsilon' j'(\epsilon', \mu', \phi'; \mathbf{r}, t'), \quad (3)$$

where primes refer to comoving quantities, the integration is over volume in the stationary (explosion) frame, the Doppler factor

$$\delta_D = \frac{1}{\Gamma(1 - \beta\mu)}, \quad (4)$$

$\beta = (1 - 1/\Gamma^2)^{1/2}$, and $\epsilon' = (1 + z)\epsilon/\delta_D$ [see Granot et al. 1999, noting the correction of a $(1 + z)$ factor in the relation between the emitted and received photon frequencies]. The emissivity

$$j_*(\epsilon_*, \Omega_*) = \frac{dE_*}{dV_* dt_* d\Omega_* d\epsilon_*} = \delta_D^2 j'(\epsilon', \Omega'),$$

where $\Omega = \Omega_*$ is the directional vector (μ, ϕ) , $\mu' = (\mu - \beta)/(1 - \beta\mu)$, and $\phi' = \phi$. We use a notation in which asterisks refer to quantities in the stationary frame (although we have dropped asterisks for the spatial variables r and Ω) and unscripted quantities refer to the observer frame.

The blast wave is assumed to emit isotropically in the comoving frame, which could apply to synchrotron and synchrotron self-Compton processes with randomly ordered magnetic fields and electron pitch-angle distributions, but not to external Compton processes. Moreover, the observer is assumed to be located along the azimuthal symmetry axis of the jet, or to be viewing a uniform jet with opening angle $\theta_j \gg 1/\Gamma$. Therefore,

$$f_\epsilon(t) = \frac{1}{2d_L^2} \int_{-1}^1 d\mu \delta_D^3 \int_0^\infty dr r^2 \epsilon' j'(\epsilon'; \mathbf{r}, t'), \quad (5)$$

noting that $\delta_D(\mathbf{r}) = \delta_D$ for a uniform jet. The emissivity is related to the internal energy density $u_{\epsilon'}(\mathbf{r}, t')$ through the relation

$$\epsilon' j'(\epsilon'; \mathbf{r}, t') \cong \frac{cu_{\epsilon'}(\mathbf{r}, t')}{\Delta r'}, \quad (6)$$

where $\Delta r' = \Gamma \Delta r$ is the proper shell width and the mean escape time of photons from the shell volume is approximated by $\Delta r'/c$.

Further consider a uniform jet with no angular dependence other than that the emission goes to zero at $\theta \geq \theta_j = \arccos \mu_j$. The emitting shell is assumed to be illuminated for the comoving duration $t'_0 \leq t' \leq t'_0 + \Delta t'$. The spectrum is approximated by a broken power law with peak νL_ν flux at energy ϵ'_{pk} , given by the expression

$$u_{\epsilon'}(\mathbf{r}, t') = u'_0 H(t'; t'_0, t'_0 + \Delta t') [x^a H(1 - x) + x^b H(x - 1)], \quad (7)$$

where H are the Heaviside functions, $a (>0)$ and $b (<0)$ are the νL_ν indices, and $x = \epsilon'/\epsilon'_{pk,0} = (1 + z)\epsilon/\delta_D \epsilon'_{pk,0}$. The peak νF_ν comoving photon energy $\epsilon'_{pk,0}$ is also supposed to be constant throughout the shell. The total integrated photon energy density for this spectrum is $u'_{tot} = u'_0(a^{-1} - b^{-1})$.

The observing time t is related to the emitting time measured in the stationary explosion frame through the relation

$$t_z = \frac{t}{1 + z} = t_* - \frac{r\mu}{c}. \quad (8)$$

The zero of time $t_* = 0$ corresponds to the moment of shell ejection, with the location of the inner edge of the shell given by the relation $r_i(t_*) = \beta c t_*$. The first moment of shell illumination takes place when the inner edge of the shell is at radius $r_0 = \beta c t_{*0} = \beta \Gamma c t'_0$ for a shell moving with constant speed Γ .

The finite shell width and finite duration of the illumination implies two constraints on the integrations over r and μ . The shell-width constraint $\beta c t_* \leq r \leq \beta c t_* + \Delta r$ implies that

$$\frac{\beta c t_z}{1 - \beta\mu} \leq r \leq \frac{\beta c t_z + \Delta r}{1 - \beta\mu}. \quad (9)$$

Because of light-travel time effects of the relativistically moving shell, values of r contributing to the signal observed at time t_z extend over a range $\Delta r/(1 - \beta\mu) \sim \Gamma^2 \Delta r$ (Rees 1966; Granot et al. 1999).

The illumination constraint $t'_0 \leq t' = t_*/\Gamma \leq t'_0 + \Delta t'$ implies that

$$\frac{1}{\mu} \left(\frac{r_0}{\beta} - c t_z \right) \leq r \leq \frac{1}{\mu} \left(\frac{r_0}{\beta} - c t_z + c \Gamma \Delta t' \right). \quad (10)$$

The zero of observer time is when a hypothetical photon ejected at $t_* = 0$ and $r = 0$ from the inner edge of the shell would reach the observer. The time at which the signal is first detected by the observer is therefore given by

$$t_z^{\text{init}} = \frac{(1 - \beta)r_0 - \Delta r}{\beta c} \rightarrow \frac{r_0}{2\Gamma^2 c} - \left(\frac{\Delta r}{c} \right),$$

and the observing time at which a photon emitted from the inner edge of the shell at the first instant of shell illumination reaches the observer is $t_{z0} = r_0(1 - \beta)/\beta c \rightarrow r_0/2\Gamma^2 c$. The final expressions in these last two relations hold in the limit $\Gamma \gg 1$. Hence,

$$f_\epsilon(t) = \frac{cu'_0}{6d_L^2 \Delta r'} \int_{\mu_j}^1 d\mu \delta_D^3 (r_u^3 - r_l^3) [x^a H(1 - x) + x^b H(x - 1)], \quad (11)$$

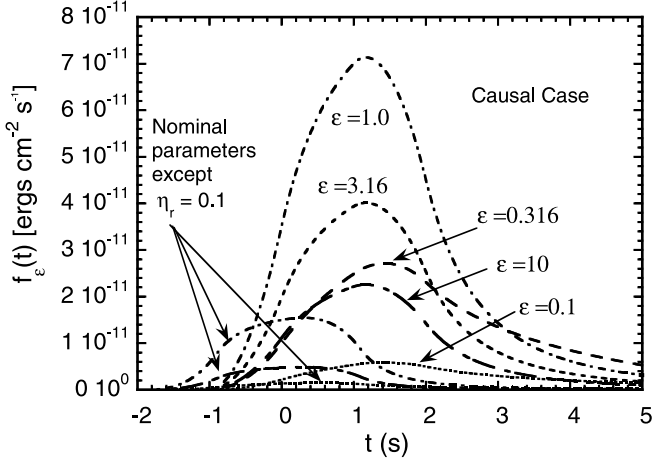


FIG. 1.—Light curves of a causal pulse at different dimensionless observing energies for a model with standard parameters (see text) and $\eta_r = \eta_t = \eta_\Delta = 1$. Also indicated by the arrows are light curves at $\epsilon = 0.1, 1.0$, and 10 for a model with $\eta_t = \eta_\Delta = 1$ and $\eta_r = 0.1$.

where

$$r_l = \max\left(\frac{\beta c t_z}{1 - \beta \mu}, \frac{r_0/\beta - c t_z}{\mu}\right)$$

and

$$r_u = \min\left(\frac{\beta c t_z + \Delta r}{1 - \beta \mu}, \frac{r_0/\beta - c t_z + c \Gamma \Delta t'}{\mu}\right).$$

3. CALCULATIONS

We examine the accuracy of the approximate expressions relating r and t_{var} (eq. [1]) and energy flux and internal energy density (eq. [2]; see Appendix A). Let t_f represent a fiducial variability timescale for the observer. We introduce radius, time, and width parameters, denoted by η_r , η_t , and η_Δ , respectively, to relate t_f to source-frame quantities. The curvature constraint for the blast-wave radius suggests that we write

$$r = 2\eta_r \Gamma^2 c t_f / (1 + z). \quad (12)$$

Because $dt' = \delta_D dt / (1 + z)$, we define

$$\Delta t' = 2\Gamma \eta_t t_f / (1 + z) \quad (13)$$

to relate the intrinsic variability timescale $\Delta t'$ in the comoving frame to t_f . The comoving width of the emitting region $\Delta r' \lesssim \Delta t' / c$, by causality requirements (if it were larger, then large-amplitude variability would not be possible except for random statistical fluctuations). Thus, we define

$$\Delta r' = 2\Gamma \eta_\Delta c t_f / (1 + z), \quad (14)$$

with the causal requirement $\eta_\Delta \lesssim \eta_t$. When $\Delta r' \ll c \Delta t'$, the duration of the emitting region is not determined by its causal size scale, but rather by the duration of emission radiated from a region much smaller than $\Delta t' / c$.

We solve equation (11) for the following standard parameters: $\Gamma = 300$; $z = 1$ (so that $d_L = 2.02 \times 10^{28}$ cm for a Λ CDM cosmology with $\Omega_m = 0.27$, $\Omega_\Lambda = 0.73$, and a Hubble constant of $72 \text{ km s}^{-1} \text{ Mpc}^{-1}$, as implied by the *WMAP* results [Spergel et al. 2003]); $\epsilon'_{\text{pk},0} = (1 + z)\epsilon_{\text{pk},0} / 2\Gamma$ with $\epsilon_{\text{pk},0} = 1$ (i.e., peak

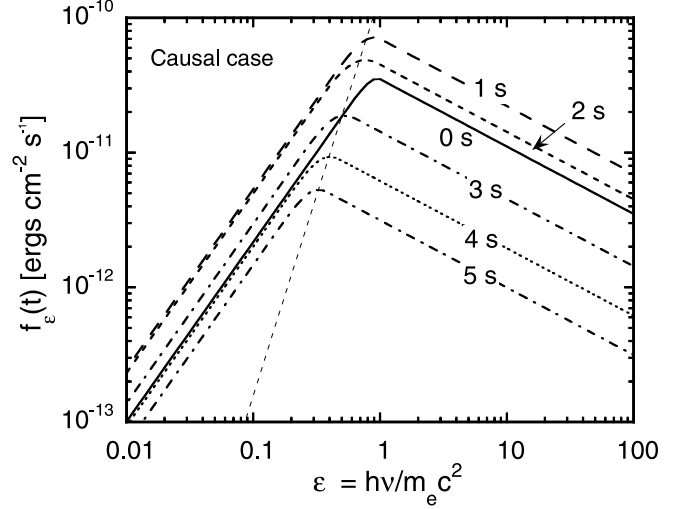


FIG. 2.—Evolution of the spectral energy distribution due to curvature effects for a model with standard parameters (see text). In the declining phase of the pulse, $f_{\text{pk}} \propto \epsilon_{\text{pk}}^3$, as indicated by the dashed line.

photon energy at the beginning of the pulse equal to 511 keV); $u'_0 = 1 \text{ ergs cm}^{-3}$; $a = 4/3$; $b = -1/2$; and $t_f = 1 \text{ s}$.

Figure 1 shows the appearance of a kinematic pulse with $\eta_r = \eta_t = \eta_\Delta = 1$ at a number of photon energies. Also shown in Figure 1 are kinematic pulses formed when $\eta_t = \eta_\Delta = 1$ and $\eta_r = 0.1$. Note the characteristic rounded, weakly asymmetric (on a linear scale) light curve shapes that are formed when $\Delta r' \cong c \Delta t'$. Time delays from different parts of the width of the emitting shell are important to determine the pulse shape in this case. The smaller emitting volume when the shell is energized at $0.1 r_0$ rather than at r_0 produces a pulse with a fluence smaller by a factor of

$$\frac{\int_{\eta_\Delta r_0}^{\eta_\Delta r_0 + c \Gamma \Delta t'} dr r^2}{\int_{r_0}^{r_0 + c \Gamma \Delta t'} dr r^2} \approx \frac{\int_{\eta_\Delta r_0}^{\eta_\Delta r_0 + r_0} dr r^2}{\int_{r_0}^{2r_0} dr r^2} \approx \frac{1.1^3 - 0.1^3}{8 - 1} \approx \frac{1}{7}.$$

Indeed, $1/7$ is the asymptotic limit of the fluence reductions due to the different volumes illuminated by flares lasting for equal proper times, but in one case emerging from deep within the jet and in the other case with the illumination beginning at the location $r_0 \cong 2\Gamma^2 c t_f / (1 + z)$. The intrinsic duration of the pulse, when combined with the curvature effects, results in a pulse with FWHM duration of $\approx 2 \text{ s}$, as compared with the fiducial timescale of 1 s . Thus, the combined width, duration, and (off-axis) curvature effects have lengthened the basic timescale by a factor of about 2 at $\epsilon \cong \epsilon_{\text{pk},0}$, with a narrower FWHM duration when $\epsilon \gtrsim \epsilon_{\text{pk},0}$ and a broader FWHM duration when $\epsilon \lesssim \epsilon_{\text{pk},0}$.

Figure 2 shows the evolution of the spectral energy distribution for this pulse. Note the rapid decay $\propto \epsilon_{\text{pk}}^3$ of the νF_ν peak flux f_{pk} measured at ϵ_{pk} during the decay portion of the pulse. This behavior is characteristic of all pulses in which curvature effects from off-axis emitting regions dominate the late-time behavior of the light curve.

Figure 3 shows characteristic light curves when $\Delta r' \ll c \Delta t'$, that is, when the shell is very thin compared with the size scale associated with the intrinsic pulse duration. These light curves exhibit pulses that have much sharper peaks than in the general case of Figure 1 and that are asymmetrical with a distinct trailing edge of emission. The fluence contained in the pulse is the same as in the pulse of Figure 1 with $\eta_r = 1$, but the FWHM pulse duration at $\epsilon = 1$ is $\approx 1 \text{ s}$, comparable to t_f ,

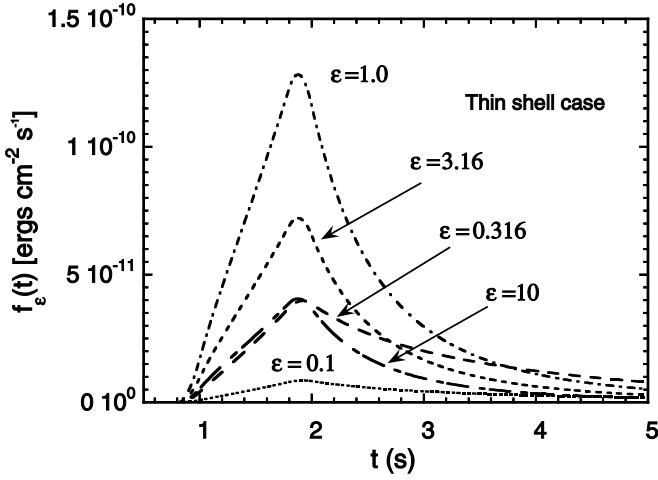


FIG. 3.—Light curves of a thin-shell pulse at different dimensionless observing photon energies for a model with $\eta_r = \eta_t = 1$ and $\eta_\Delta = 0.1$, so that the shell width $\Delta r' = 0.1 \Delta t'/c$.

while the peak flux is about twice as large, as a result of the different geometry. The difference in the geometries of causal and thin-shell pulses introduces a physical effect required for accurate calculations of scattering or opacity processes in GRB blast waves. When $\Delta r' \approx c \Delta t'$, then the photon field can be considered to be roughly isotropic for scattering and opacity calculations. But when the shell radiates for a much longer time than it takes light to cross the width of the shell, that is, when $\Delta t' \gg \Delta r'/c$, the geometry of the outflowing photon flux is much more anisotropic, giving higher thresholds and lower rates for $\gamma\gamma$ and photohadronic processes as a result of the reduction in the frequency of head-on collisions.

Figure 4 shows the characteristic light-curve shapes formed when curvature effects dominate the temporal evolution of the light curve (Fenimore et al. 1996). Here the pulses are very asymmetric, with a sharp leading edge. In this calculation, $\eta_r = 1$ and $\eta_\Delta = \eta_t = 0.1$. The peak νF_ν flux at $\epsilon = 1$ reaches a value of only 1.4×10^{-11} ergs s $^{-1}$ with a duration of ≈ 0.4 s. The total energy released is smaller by a factor of 10 than in the case shown in Figures 1 and 2 with $\eta_r = 1$, as a result of the shorter intrinsic pulse duration.

The bottom panel in Figure 4 shows, in a log-log relation, that the flux decays as t^{-3+b} at $\epsilon > \epsilon_{\text{pk}}$. When $\epsilon < \epsilon_{\text{pk}}$, the flux decays as t^{-3+a} at early times, breaking to a t^{-3+b} behavior at late times because of curvature effects.

The spectral and temporal behavior of the curvature pulse can be derived in the δ -function approximation (not to be confused with the Doppler factor δ_D). If we let

$$\begin{aligned} \epsilon' j'(\epsilon'; \mathbf{r}, t') &\propto \epsilon'^a \delta(r' - r_0) \delta(t' - t'_0) \\ &= \epsilon'^a \delta(r - r_0) \delta\left[t - \frac{(1+z)t'_0}{\delta_D}\right] \end{aligned}$$

in equation (5) and use the invariance of the 4-volume, then

$$\begin{aligned} f_\epsilon(t) &\propto \frac{r_0^2}{2d_L^2} \epsilon^a \int d(1 - \beta\mu) \delta_D^{-3-a} \delta\left[(1 - \beta\mu) - \frac{t_z}{\Gamma t'_0}\right] \\ &\propto \epsilon^a \left(\frac{\beta c t_z}{r_0}\right)^{-3+a} \propto \epsilon^a \left(\frac{\beta c t_z}{r_0}\right)^{-2-\alpha}, \end{aligned} \quad (15)$$

where $t'_0 = r_0/\beta\Gamma c$ and α is the energy index. [This result corrects the expressions given by Fenimore et al. 1996 and Ryde

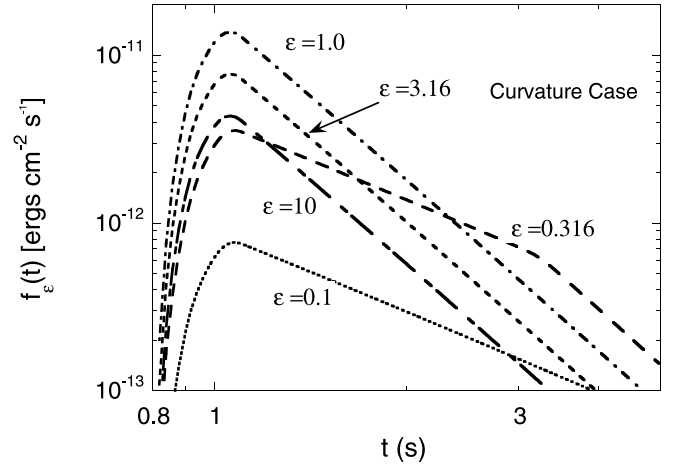
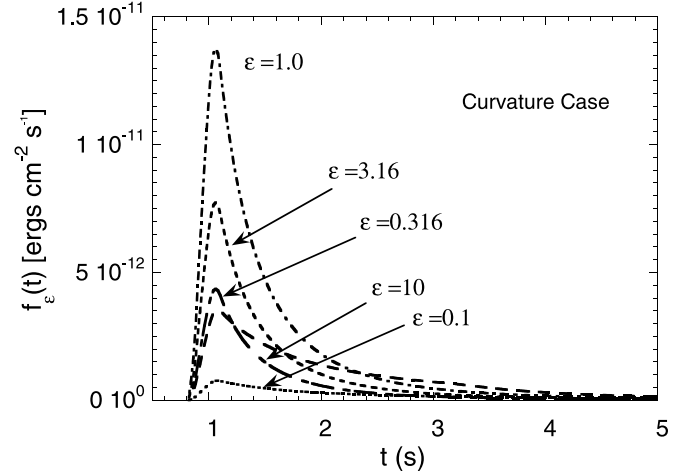


FIG. 4.—Light curves of a curvature pulse at different dimensionless observing photon energies for a model with $\eta_r = 1$, but with $\eta_\Delta = \eta_t = 0.1$.

& Petrosian 2002, where the δ -function pulse in time, $\delta(t' - t'_0)$, is not transformed between the comoving and observer frames.] The dependence in equation (15) is derived more carefully in Appendix B, and analytic forms for the pulse profile, including a simple functional form for the pulse profile in the curvature limit, are derived in Appendix C.

4. DISCUSSION

The estimate $L \cong 4\pi d_L^2 \Phi_E \cong 4\pi r_0^2 c u'_0 \Gamma^2$, where the received flux is intensified by 2 powers of Γ for the relativistic time contraction and photon energy enhancement in a blast-wave geometry, is generally used to relate bolometric energy flux and internal energy density (Appendix A). More remarkably, the allowed radius of the radiating spherical shell is $\approx 2\Gamma^2$ times larger than inferred through causality arguments applied to the measured variability timescale. This effect greatly dilutes the comoving photon density compared with that of a stationary emitting region and essentially explains the unusual properties of GRBs. In total, we see that

$$\Phi_E \cong \frac{c r_0^2 u'_0 \Gamma^2}{d_L^2} = \frac{4c^3 t_{\text{var}}^2}{(1+z)^2 d_L^2} u'_0 \Gamma^6 \propto u'_0 \Gamma^6. \quad (16)$$

For the nominal parameters used in the figures, $\Phi_E \cong 4.8 \times 10^{-11} t_{\text{var}}^2 u'_0 \Gamma^6$ ergs cm $^{-2}$ s $^{-1}$, where t_{var} is in seconds and u'_0 is in units of ergs cm $^{-3}$.

The most rigorous limits on $\gamma\gamma$ attenuation are obtained by determining the *minimum value* of the product $u'_0\Delta t'$ that can produce a pulse with a measured peak flux f_{pk} and full width at half-maximum (FWHM) duration $t_{1/2}$ for a given value of Γ . It is the product $u'_0\Delta t'$ that enters into the $\gamma\gamma$ attenuation (and photomeson) calculations. If the shell is found to be optically thick at some photon energy for a given value of Γ even in this case, then Γ must be larger if photons with the corresponding energies are detected.

Inspection of the various cases shows that the pulse formed in the curvature limit produces the brightest measured flux and shortest duration for a given value of the product $u'_0\Delta t'$. This is because the measured duration is due entirely to curvature effects, and the radiated energy is compressed into the shortest duration and brightest pulse in this limit. From the results of Appendices C and D, this implies that the expression

$$u'_0\Delta t' \cong \frac{(2^{1/(3-a)} - 1)(1+z)d_L^2 f_{\text{pk}}}{8c^3 \Gamma^5 t_{1/2}} \quad (17)$$

gives the smallest possible values for $u'_0\Delta t'$, and this expression will therefore yield the most reliable minimum Lorentz factors for $\gamma\gamma$ attenuation calculations derived from *GLAST* or ground-based air Cerenkov telescope observations. The corresponding expression for the comoving photon spectral energy density is thus

$$u'_{\epsilon'} \cong \frac{0.26(1+z)d_L^2 f_{\text{pk}}}{8c^3 \Gamma^5 t_{1/2} \Delta t'} [x^a H(1-x) + x^b H(x-1)], \quad (18)$$

where $t_{1/2}$ is determined at photon energies near the peak of the νF_ν spectrum. Equation (18) is a factor of 3 smaller than the expression used for a comoving spherical blob with $\delta \rightarrow \Gamma$ and $t_{\text{var}} \rightarrow t_{1/2}$ (see eq. [2] in Dermer 2004).

Three generic types of pulses have been identified for the simple kinematic pulse, namely, the curvature case, in which $r_0 \gg c\Gamma\Delta t'$, the causal case, in which $r_0 \approx \Gamma\Delta r' \approx c\Gamma\Delta t'$, and the thin shell case, in which $\Delta r' \ll c\Delta t'$. In all three types of kinematic pulses, curvature effects dominate the formation of the spectrum at late time $t \gg (1+z)\Delta t'/2\Gamma$, so that $f_{\text{pk}} \propto \epsilon_{\text{pk}}^3$ if curvature effects dominate pulse formation at late times.

The curvature relationship can be derived from a simple scaling argument by noting that the differential stationary-frame shell volume that contributes to the received flux, given by $dV = 2\pi r_0^2 \Delta r d\mu$, remains constant with time. This is because the relation between reception time t and μ for a shell that is instantaneously illuminated at comoving time t'_0 is $t = (1+z)\Gamma t'_0(1-\beta\mu)$, so that $d\mu \propto dt$. The νF_ν flux

$$f_\epsilon = \frac{\delta_D^4 L'}{4\pi d_L^2} = \frac{\delta_D^4 V' \epsilon' j(\epsilon')}{4\pi d_L^2} = \frac{\delta_D^3 V \epsilon' j(\epsilon')}{4\pi d_L^2},$$

where L' is the comoving luminosity of the emitting volume that contributes to the flux at time t . For an emission spectrum that is flat, that is, $\epsilon' j(\epsilon') \propto \epsilon'^0$, $f_{\text{pk}} \propto \epsilon_{\text{pk}}^3$, because $\epsilon_{\text{pk}} \propto \delta$ for a uniform shell.

Analysis of BATSE GRB light curves (Borgonovo & Ryde 2001) shows that the peak fluxes of a GRB pulse generally follow a relation whereby

$$f_{\text{pk}} \propto \epsilon_{\text{pk}}^\zeta. \quad (19)$$

Values of ζ for different GRBs vary over a wide range from ≈ 0.6 to 3, with values of ζ roughly constant for pulses within the same GRB or in a GRB consisting of a single smooth pulse. In most GRBs, therefore, curvature effects do not make a large contribution to the decay phase of a GRB light curve.

An interesting question is the source of the difference between observations and our kinematic model pulses. One possibility is that the jet has angular structure and varies with directional energy release and baryon loading on angles θ of a few times Γ^{-1} . The angle-dependent speeds in such a system would produce a deformed, colliding, shocked-fluid shell in which the spherical symmetry assumption fails, as therefore would the uniform jet model. If this is the case, then GRB prompt emission data can in principle be analyzed to reveal shell structure and to determine whether this behavior is consistent with a universal jet structure (Zhang et al. 2004; see Frail 2004 for a review).

Rather than treat these geometrical effects here, we consider instead whether radiation effects could form a power-law relation between f_{pk} and ϵ_{pk} . The most naive system considers a fixed volume of shocked fluid within which the peak of the νF_ν spectrum is made by a large population of quasi-monoenergetic electrons that radiates most of the power through the synchrotron process in a mean magnetic field of strength B . If these electrons mainly have comoving Lorentz factors γ , then their luminous power is $\propto B^2 \gamma^2$. Because the peak of the νF_ν spectrum is $\propto B \gamma^2$, and assuming that B is constant, then $f_{\text{pk}} \propto \epsilon_{\text{pk}}$ or $\zeta_{\text{syn}} = 1$ for this simple synchrotron model with constant magnetic field. This model can therefore only apply in rare cases.

A better treatment must consider the evolution of γ due to synchrotron and adiabatic losses in the expanding shell. The equation of electron energy evolution is given by

$$-\frac{d\gamma}{dt'} = \frac{1}{V'_{\text{sh}}} \frac{dV'_{\text{sh}}}{dt'} \frac{\gamma}{3} + \frac{\sigma_T B^2(t')}{6\pi m_e c} \gamma^2, \quad (20)$$

where the comoving shell volume changes with time according to $V'_{\text{sh}} \propto t'^{3m}$, with $m = 0$ corresponding to no expansion, and $m = 1$ corresponding to three-dimensional expansion.

The magnetic field will also change as a result of the expansion of the shell volume. In the flux-freezing limit where the magnetic field is randomly oriented, $BR^2 \propto \text{constant}$, implying that $B \propto V'^{1/3} \propto t'^{-2m}$. The well-ordered magnetic field required to explain the polarization observation of GRB 021206 observed with *RHESSI* (Coburn & Boggs 2003) suggests that there is not an efficient mixing and randomization of the magnetic field directions. For simplicity, we therefore write $B \propto t'^{-2vm}$, where $v = 1$ gives the flux-freezing limit.

Equation (20) becomes

$$-\frac{d\gamma}{d\tau} = m \frac{\gamma}{\tau} + \nu_0 \tau^{-4vm} \gamma^2, \quad (21)$$

where $\tau \geq 1$ is a dimensionless time variable and ν_0 is a dimensionless synchrotron energy loss rate. Equation (21) is analytic, but it is sufficient to consider two limiting cases of dominant adiabatic losses or dominant synchrotron losses at late times. In the case of dominant adiabatic losses we have (dropping the primes) $\gamma \propto t^{-m}$, $B \propto t^{-2vm}$, and $\epsilon_{\text{pk}} \propto t^{-2m(1+v)}$, so that $f_{\text{pk}}/\epsilon_{\text{pk}} \propto B \propto \epsilon_{\text{pk}}^{v/(v+1)}$. Thus, $\zeta_{\text{adi}} = 1 + v/(v+1)$. Even

for a wide range of values of v , $1 \lesssim \zeta_{\text{adi}} \lesssim 2$, and ζ_{adi} is independent of the geometry factor m .

If synchrotron losses dominate the cooling, $-d\gamma/dt \propto B^2\gamma^2$. The dependence $B \propto t^{-2vm}$ therefore implies $\gamma \propto t^{4vm-1}$, so that $\epsilon_{\text{pk}} \propto B\gamma^2 \propto t^{6vm-2}$. Hence, $f_{\epsilon_{\text{pk}}}/\epsilon_{\text{pk}} \propto B \propto \epsilon_{\text{pk}}^{vm/(1-3vm)}$, so that $\zeta_{\text{syn}} = 1 + vm/(1 - 3vm)$. Except when $v \ll 1$, $\zeta_{\text{syn}} \approx 1$ when $m = 0$ and $\zeta_{\text{syn}} \approx 0.5 - 0.67$ when $m = 1$. In this simple model, therefore, values of ζ between $1/2$ and $2/3$ are only possible for three-dimensional expansion.

Three-dimensional expansion is more likely to occur for narrowly collimated blast waves than for blast waves with large opening angles, and the narrowly collimated blast waves would have “beaming breaks” in the optical afterglow light curves at earlier times. If we conjecture that the $f_{\epsilon_{\text{pk}}}/\epsilon_{\text{pk}}$ relationships are due to synchrotron and adiabatic effects in GRB blast waves with different opening angles, then those blast waves with $\zeta < 1$ should be correlated with earlier beaming break times. Because this effect is only seen when synchrotron losses dominate the cooling, GRBs with $\zeta < 1$ should also display cooling spectra with photon indices $\approx 3/2$ below ϵ_{pk} .

Borgonovo & Ryde (2001) find several GRBs and many pulses in the BATSE sample with statistically significant values of ζ less than unity. These GRBs, however, preceded the afterglow era. Of those GRBs that have measured beaming breaks (see Table 1 in Bloom et al. 2003), only GRB 990123 has sufficiently bright BATSE data to provide a data point for such a correlation. GRB 990123 has not yet been analyzed to give ζ , while analysis of *BeppoSAX* data is in progress (F. Ryde 2004, private communication).

Such a model for the $f_{\epsilon_{\text{pk}}}/\epsilon_{\text{pk}}$ relationship would explain why ζ is approximately constant for different pulses within a GRB, provided that the opening angle of the GRB jet remains the same throughout the period of activity of the GRB engine.

The adiabatic/synchrotron model would not, however, explain pulses with $2 \lesssim \zeta \lesssim 3$. There are many such pulses in the Borgonovo & Ryde (2001) sample, although generally with large error bars. If analyses of *BeppoSAX* or *Swift* data reveal such GRBs, then another explanation is required. One possibility is that GRB pulses are due to the interactions of a single impulsive blast wave with inhomogeneities in the surrounding medium. This version of the external shock model for the prompt phase can be much more efficient than an internal shell model (Dermer & Mitman 1999, 2004) and permits quantitative studies of the statistics of BATSE GRBs (Böttcher & Dermer 2000; see Zhang & Mészáros 2004 for a review of the internal/external controversy).

Predictions for the $f_{\epsilon_{\text{pk}}}/\epsilon_{\text{pk}}$ relationship in an external shock model (Dermer et al. 1999b) can be derived by adapting the equations for blast-wave deceleration in a uniform medium with $\Gamma = \Gamma_0/[1 + (x/x_d)^g]$, where Γ_0 is the initial Lorentz factor, x_d is the deceleration distance, and g is the radiative index ($g = 3/2$ and 3 for an adiabatic and a fully radiative blast wave, respectively). In the deceleration phase, $x \propto t^{1/(2g+1)}$, and therefore $\Gamma \propto t^{-g/(2g+1)}$. In this model, $\epsilon_{\text{pk}} \propto \Gamma B \gamma_{\text{pk}}^2$ and $f_{\epsilon_{\text{pk}}} \propto \Gamma^2 B^2 \gamma_{\text{pk}}^2$, where $\gamma_{\text{pk}} \propto \Gamma^4 \propto t^{-4g/(2g+1)}$ in the slow-cooling regime and $\gamma_{\text{pk}} \propto (x\Gamma)^{-1} \propto t^{-2/(2g+1)}$ in the fast-cooling regime. Thus, $f_{\epsilon_{\text{pk}}}/\epsilon_{\text{pk}} \propto B\Gamma$.

In the slow-cooling regime, $\epsilon_{\text{pk}} \propto \Gamma^4 \propto t^{-4g/(2g+1)}$ and $f_{\epsilon_{\text{pk}}} \propto \epsilon_{\text{pk}}^{3/2}$. In the fast-cooling regime, $\epsilon_{\text{pk}} \propto t^{-2/(2g+1)}$ and $f_{\epsilon_{\text{pk}}} \propto \epsilon_{\text{pk}}^{1+g}$. In the slow-cooling and fast-cooling regimes, therefore, values of $\zeta_{\text{sc}} = 3/2$ and $\zeta_{\text{fc}} = 1 + g$, respectively, are predicted. Provided that the surrounding medium is uniform (which can be

inferred from afterglow modeling, though at a larger distance scale), the slow-cooling result implies a definite value of $\zeta_{\text{sc}} = 3/2$ for fast-rise, smooth-decay light curves when spectral analysis demonstrates that the GRB evolves in the slow-cooling regime. For GRBs in fast-cooling regime, this estimate implies that $5/2 < \zeta_{\text{fc}} < 4$, and in these cases cooling spectra should be apparent. Further work is needed to extend the results to radial density gradients of the circumburst medium and to verify that these relations hold for deceleration in small density inhomogeneities that form GRB pulses in the external shock model.

5. SUMMARY

A simple kinematic model for GRB colliding shells has been constructed that provides a framework for analyzing radiative processes in a simplified geometry of a thin or thick shell traveling at relativistic speeds. The relationship between observed flux and comoving photon energy density for a given value of Γ has been studied, showing that the curvature limit yields the smallest value of the product $u'_0 \Delta t'$. This result can then be used to deduce conservative lower limits on bulk Lorentz factors derived from the condition of $\gamma\gamma$ transparency.

The kinematic model predicts the curvature relationship $f_{\epsilon_{\text{pk}}} \propto \epsilon_{\text{pk}}^\zeta$, with $\zeta = 3$, at late times in GRB pulses. Equivalently, curvature effects imply that $f_\epsilon(t) \propto t^{-3+a}$ and $\epsilon_{\text{pk}} \propto t^{-1}$. BATSE data for GRB pulses do not display the curvature relationship in most cases (Borgonovo & Ryde 2001), suggesting that the physics of pulse formation is dominated by other effects. A simple model for joint evolution of $f_{\epsilon_{\text{pk}}}$ and ϵ_{pk} that takes into account adiabatic and synchrotron losses implies that $1/2 < \zeta < 2$ and that $\zeta \approx 0.5$ only when the shell undergoes three-dimensional expansion and the electrons that produce the emission near ϵ_{pk} are rapidly cooling through synchrotron losses. Spectral analysis of *Swift* data and correlations of ζ with times of the beaming breaks in optical afterglow light curves can test this prediction. Such a correlation would validate an adiabatic/synchrotron model for GRB prompt radiation, relate properties of the prompt phase with the afterglow, and provide key insights into the properties of GRB jets.

Another possibility is that the $f_{\epsilon_{\text{pk}}} \propto \epsilon_{\text{pk}}^\zeta$ relationship is formed by external shock processes, and a simple derivation of ζ was given for blast-wave deceleration in a uniform surrounding medium. Analysis of prompt data has the potential to test the external shock model, although complications regarding density gradients and inhomogeneities in the circumburst medium must be considered in more detail.

A final possibility is that jet structure produces the measured relationship between $f_{\epsilon_{\text{pk}}}$ and ϵ_{pk} . The validity of a universal jet model will be tested by determining whether observed values of ζ can derive from the proposed angle dependence. In the meantime, comparing the predictions of the adiabatic/synchrotron and external shock models with time-resolved spectroscopy of GRB pulses and afterglows has the potential to rule out or validate these models.

I thank Markus Böttcher, Felix Ryde, and the anonymous referee for valuable comments. This work is supported by the Office of Naval Research and NASA *GLAST* Science Investigation grant DPR S-13756G.

APPENDIX A

RELATIONS AND ESTIMATES

First we relate the total energy in photons between the comoving and stationary frames. The differential number of photons $N_*(\epsilon_*, \Omega_*)$ per unit energy and solid angle transforms as $N_*(\epsilon_*, \Omega_*) = \delta_D N'(\epsilon', \Omega')$, as is easily seen by calculating the Jacobian of the transformation or by noting that $\epsilon^{-1} dN/d\epsilon d\Omega \equiv \epsilon^{-1} N(\epsilon, \Omega)$ is an invariant. For an isotropic, monochromatic photon spectrum in the comoving frame, $N'(\epsilon', \Omega') = N_0 \delta(\epsilon' - \epsilon'_0)/4\pi$, and the total photon energy in the comoving frame is just $E'_0 = N_0 \epsilon'_0$ (in units of the electron rest mass). The differential photon spectrum in the stationary frame is therefore $N_*(\epsilon_*, \Omega_*) = \delta N_0 \delta(\epsilon_*/\delta_D - \epsilon'_0)/4\pi = \delta_D^2 N_0 \delta(\epsilon_* - \delta_D \epsilon'_0)/4\pi$, so that

$$E_* = \oint d\Omega_* \int_0^\infty d\epsilon_* \epsilon_* N_*(\epsilon_*, \Omega_*) = \frac{N_0 \epsilon'_0}{2} \int_{-1}^1 d\mu \delta_D^3 = \Gamma E'. \quad (\text{A1})$$

This result is obvious by noting the symmetry of the transformation equation $\epsilon_* = \Gamma \epsilon' (1 + \beta \mu')$ with respect to μ' .

Because $\Phi_E = L/4\pi d_L^2$, by definition of the luminosity distance d_L , the fluence $\varphi = \Phi_E \langle t \rangle = L_* \langle t \rangle / 4\pi d_L^2 = L_* \langle t \rangle (1+z) / 4\pi d_L^2$, where $\langle t \rangle$ and $\langle t_* \rangle$ are the times of reception and emission in the observer and stationary frame, respectively. Using equation (A1) gives

$$\varphi = \frac{\Gamma E'}{4\pi d_L^2} (1+z). \quad (\text{A2})$$

This expression only holds when the emission is isotropic in the comoving frame.

A simple estimate relating comoving energy density u'_0 with energy flux Φ_E is obtained by noting that the stationary frame luminosity of a blast wave is given by $L_* = dE_*/dt_* = \Gamma^2 L'$, where $L' = dE'/dt' \cong u'_0 4\pi r^2 \Delta r' / (\Delta r'/c)$. Thus, $\Phi_E \cong cr^2 u'_0 \Gamma^2 / d_L^2$, giving equation (2). If the variability is produced by curvature effects according to equation (1), then

$$\Phi_E = \frac{4c^3 u'_0 \Gamma^6 t_{\text{var}}^2}{(1+z)^2 d_L^2}. \quad (\text{A3})$$

Note that the same basic dependence, though with Γ replaced by δ , is derived for a (comoving) spherical blob geometry. In this case, $\Phi_E \cong \delta_D^4 L' / 4\pi d_L^2$, and $L' \cong 4\pi r_b^2 c u'_0 / 3$, with blob radius $r_b' = c \delta_D t_{\text{var}} / (1+z)$.

APPENDIX B

ANALYTIC DERIVATION OF THE $f_{\epsilon_{\text{pk}}}(t)$ VERSUS ϵ_{pk} RELATION

Starting with equation (5), we approximate

$$\epsilon' j'(\epsilon'; \mathbf{r}, t') = K \epsilon'^a \delta(r' - r_0) \delta(t' - t'_0) H(\epsilon'; \epsilon'_l, \epsilon'_u). \quad (\text{B1})$$

Normalizing to the comoving energy E'_p of a pulse implies that

$$K = \frac{a E'_p}{2\pi (1 - \mu_j) r_0^2 (\epsilon_u'^a - \epsilon_l'^a)}. \quad (\text{B2})$$

The integrals can now be performed. First note the subtlety that $|dr/dr'| = \delta_D$, whereas $\Delta r' = \Gamma \Delta r$ in equation (6). Imposing the limits over r in equation (9) recovers the δ_D factor in the numerical integration of equation (11) performed in § 2. Further noting that $t'_0 = r_0/\beta\Gamma c$, and defining $\epsilon_z = (1+z)\epsilon$, we obtain

$$f_\epsilon(t) = \frac{K c r_0 \epsilon_z^a}{2 d_L^2} \left(\frac{\beta \Gamma c t_z}{r_0} \right)^{-3+a} H \left[\frac{\beta c t_z}{r_0}; \max \left(1 - \beta, \frac{\epsilon'_l}{\Gamma \epsilon_z} \right), \min \left(1 - \beta \mu_j, \frac{\epsilon'_u}{\Gamma \epsilon_z} \right) \right] \propto \epsilon_z^a t_z^{-3+a}. \quad (\text{B3})$$

The final proportionality holds provided that t_z is in the range satisfying the Heaviside function. When $a = 0$, corresponding to emission at the peak of the νF_ν spectrum, $f_{\epsilon_{\text{pk}}}(t) \propto t_z^{-3} \propto \epsilon_{\text{pk}}^3$. This follows because $\epsilon_{\text{pk}} \propto t_z^{-1}$, as is apparent by inspecting the limits in the Heaviside function ($\beta c t_z / r_0 \propto \epsilon'_u / \Gamma \epsilon_z$, so that $\epsilon_{\text{pk}} \propto \epsilon'_{\text{pk}} / t_z$).

The validity of equation (B3) can be checked by deriving the fluence $\varphi = \int_0^\infty d\epsilon \int_{-\infty}^\infty dt f_\epsilon(t) / \epsilon$, using the normalization in equation (B2), from which equation (A2) is recovered.

APPENDIX C

RELATIONSHIP BETWEEN $f_\epsilon(t)$ AND u'_0 IN THE CURVATURE LIMIT

We now derive an approximate analytic expression for a radiation pulse in the curvature limit. Substituting equations (6) and (7) for the comoving spectral energy density into equation (5), the r -integral can be approximately solved by letting $\int dr r^2(\dots)/\Delta r' \rightarrow r_0^2 |dr/dr'|(\dots) \cong \delta_D r_0^2(\dots)$. In the limit $\Gamma \gg 1$, one obtains

$$f_\epsilon(t) = \frac{4cu'_0 r_0^2 \Gamma^2}{d_L^2} \left[\frac{(\epsilon/\epsilon_{\text{pk},0})^a}{3-a} Q_a + \frac{(\epsilon/\epsilon_{\text{pk},0})^b}{3-b} Q_b \right], \quad (\text{C1})$$

where

$$Q_a = \left[\max\left(1, \frac{u}{1+\eta}\right) \right]^{-3+a} - \left[\min\left(4\Gamma^2, u, \frac{\epsilon_{\text{pk},0}}{\epsilon}\right) \right]^{-3+a}, \quad (\text{C2})$$

$$Q_b = \left[\max\left(1, \frac{u}{1+\eta}, \frac{\epsilon_{\text{pk},0}}{\epsilon}\right) \right]^{-3+b} - \left[\min(4\Gamma^2, u) \right]^{-3+b}, \quad (\text{C3})$$

$u \equiv 2\Gamma^2 ct_z/r_0$, $\eta \equiv \Gamma c \Delta t'/r_0 = \eta_t/\eta_r$, and we set $\mu_j = -1$ [otherwise the terms $4\Gamma^2$ are replaced with $2\Gamma^2(1 - \beta\mu_j)$ in eqs. (C2) and (C3) above]. The νF_ν peak energy observed at the start of the pulse is denoted by $\epsilon_{\text{pk},0} = 2\Gamma \epsilon'_{\text{pk},0}/(1+z)$.

By examining the limits in equation (C2), one finds that

$$Q_a = \begin{cases} 1 - u^{-3+a}, & 1 \leq u \leq \frac{\epsilon_{\text{pk},0}}{\epsilon} \leq 1 + \eta, \\ 1 - \left(\frac{\epsilon_{\text{pk},0}}{\epsilon}\right)^{-3+a}, & 1 \leq \frac{\epsilon_{\text{pk},0}}{\epsilon} \leq u \leq 1 + \eta, \\ \left(\frac{u}{1+\eta}\right)^{-3+a} - \left(\frac{\epsilon_{\text{pk},0}}{\epsilon}\right)^{-3+a}, & 1 \leq \frac{u}{1+\eta} \leq \frac{\epsilon_{\text{pk},0}}{\epsilon} \leq u, \\ \left(\frac{u}{1+\eta}\right)^{-3+a} - u^{-3+a}, & 1 + \eta \leq u \leq \frac{\epsilon_{\text{pk},0}}{\epsilon}, \end{cases} \quad (\text{C4})$$

with related expressions for Q_b . In the limit $\eta \ll 1$, corresponding to the curvature limit where variability arises principally from curvature effects, the fourth relation in equation (C4) applies, giving

$$f_\epsilon \cong \frac{4cu'_0 r_0^2 \Gamma^2}{d_L^2} \eta \left[\left(\frac{\epsilon}{\epsilon_{\text{pk},0}}\right)^a u^{-3+a} H\left(\frac{\epsilon_{\text{pk},0}}{u} - \epsilon\right) + \left(\frac{\epsilon}{\epsilon_{\text{pk},0}}\right)^b u^{-3+b} H\left(\epsilon - \frac{\epsilon_{\text{pk},0}}{u}\right) \right]. \quad (\text{C5})$$

This expression applies equally to the late-time asymptote $t \gg (1+z)\Delta t'/2\Gamma$. At the peak of the νF_ν spectrum, $a = 0$, and

$$f_{\epsilon_{\text{pk}}} = \frac{4cu'_0 r_0^2 \Gamma^2}{d_L^2} \eta \left(\frac{2\Gamma^2 ct_z}{r_0} \right)^{-3}, \quad (\text{C6})$$

recovering the dependence derived in equation (B3). Note that because $r_0 \propto \eta_r$, $f_\epsilon \propto \eta_r \eta_t$. Equation (C5) relates $f_\epsilon(t)$ and u'_0 in the curvature limit.

APPENDIX D

SEARCHING FOR CURVATURE EFFECTS IN GRB PULSES

If the GRB spectral flux is described by a power-law spectrum with νF_ν index a , then curvature effects in the curvature limit would produce the behavior

$$f_\epsilon(t) \propto t_z^{-3+a}. \quad (\text{D1})$$

The FWHM duration of the curvature spectrum in such a regime is given by $t_{1/2} = (2^{1/(3-a)} - 1)t_{\text{pk}}$, where $t_{\text{pk}} = (1+z)r_0/2\Gamma^2 c$. Hence, the expression $r_0 = 2\Gamma^2 ct_{\text{FWHM}}/[(2^{1/(3-a)} - 1)(1+z)]$ relates the blast-wave radius r_0 to Γ , given the observables z and t_{FWHM} —provided that the pulse shape is determined by curvature effects. Curvature effects also dictate that $f_{\epsilon_{\text{pk}}} \propto \epsilon_{\text{pk}}^3$. By examining the variation of intensity as a function of ϵ_{pk} for two GRBs, Soderberg & Fenimore (2001) searched for the signature of shell curvature using an expression analogous to equation (D1), although without success. In this case, $f_{\epsilon_{\text{pk}}} \propto \epsilon_{\text{pk}}^{3-\langle a+b \rangle}$, where $\langle a+b \rangle$ is the mean index of the photon flux within the interval containing ϵ_{pk} used to measure $f_{\epsilon_{\text{pk}}}$ (to first order, $\langle a+b \rangle = 0$).

Equation (C6) can be used to derive an expression relating ϵ_{pk} to the photon fluence φ in the curvature limit. One simply obtains

$$\frac{\epsilon_{\text{pk}}}{\epsilon_{\text{pk},0}} = \sqrt{1 - \frac{\varphi}{\varphi_{\text{tot}}}}, \quad (\text{D2})$$

where $\epsilon_{\text{pk},0}$ refers to the value of ϵ_{pk} at the beginning of the pulse and φ_{tot} refers to the total fluence. This expression represents an alternative analytic form to the relation $\epsilon_{\text{pk}}/\epsilon_{\text{pk},0} = \exp(-\varphi/\varphi_{\text{tot}})$ proposed by Liang & Kargatis (1996) and also derives from equation (C5), provided that a and b are independent of time. A more general fitting function is obtained by raising the right-hand side of equation (D2) to an arbitrary power.

When equation (D2) deviates from observational data, as will often be the case since the approximations leading to the curvature pulse are rarely expected to be realized in GRB colliding shells, then curvature effects can still be sought by numerically evaluating equations (11) or (C1) to obtain more general $\epsilon_{\text{pk}}-\varphi$ relations. These equations can also be used to fit pulse profiles directly. Such an approach would place the phenomenological treatments of Kocevski et al. (2003) and Ryde et al. (2003) on a physical basis and can be extended to treat realistic electron injection and loss processes. Such results can then be compared with predictions of the external shock models for the prompt phase.

REFERENCES

- Bloom, J. S., Frail, D. A., & Kulkarni, S. R. 2003, *ApJ*, 594, 674
 Borgonovo, L., & Ryde, F. 2001, *ApJ*, 548, 770
 Böttcher, M., & Dermer, C. D. 2000, *ApJ*, 529, 635
 Coburn, W., & Boggs, S. E. 2003, *Nature*, 423, 415
 Daigne, F., & Mochkovitch, R. 1998, *MNRAS*, 296, 275
 Dermer, C. D. 2004, in *Proc. Tenth Marcel Grossmann Meeting on General Relativity*, ed. M. Novello, S. Perez-Bergliaffa, & R. Ruffini (Singapore: World Scientific), in press (astro-ph/0402438)
 Dermer, C. D., Böttcher, M., & Chiang, J. 1999a, *ApJ*, 515, L49
 Dermer, C. D., Chiang, J., & Böttcher, M. 1999b, *ApJ*, 513, 656
 Dermer, C. D., & Mitman, K. E. 1999, *ApJ*, 513, L5
 ———. 2004, in *ASP Conf. Ser. 312, Third Rome Workshop on Gamma Ray Bursts in the Afterglow Era*, ed. M. Feroci, F. Frontera, N. Masetti, & L. Piro (San Francisco: ASP), 301
 Fenimore, E. E., Madras, C. D., & Nayakshin, S. 1996, *ApJ*, 473, 998
 Frail, D. A. 2004, *Nucl. Phys. B*, 132, 255
 Frail, D. A., et al. 2001, *ApJ*, 562, L55
 Granot, J., Piran, T., & Sari, R. 1999, *ApJ*, 513, 679
 Kobayashi, S., Piran, T., & Sari, R. 1997, *ApJ*, 490, 92
 Kocevski, D., Ryde, F., & Liang, E. 2003, *ApJ*, 596, 389
 Liang, E., & Kargatis, V. 1996, *Nature*, 381, 49
 Lithwick, Y., & Sari, R. 2001, *ApJ*, 555, 540
 Rees, M. 1966, *Nature*, 211, 468
 Rybicki, G. B., & Lightman, A. P. 1979, *Radiative Processes in Astrophysics* (New York: Wiley-Interscience)
 Ryde, F., Borgonovo, L., Larsson, S., Lund, N., von Kienlin, A., & Lichti, G. 2003, *A&A*, 411, L331
 Ryde, F., & Petrosian, V. 2002, *ApJ*, 578, 290
 Soderberg, A. M., & Fenimore, E. E. 2001, in *Gamma-Ray Bursts in the Afterglow Era*, ed. E. Costa, F. Frontera, & J. Hjorth (Berlin: Springer), 87
 Spergel, D. N., et al. 2003, *ApJS*, 148, 175
 Waxman, E., & Bahcall, J. 1997, *Phys. Rev. Lett.*, 78, 2292
 Zhang, B., Dai, X., Lloyd-Ronning, N. M., & Mészáros, P. 2004, *ApJ*, 601, L119
 Zhang, B., & Mészáros, P. 2004, *Int. J. Mod. Phys. A*, 19, 2385